This full text paper was peer reviewed at the direction of IEEE Communications Society subject matter experts for publication in the IEEE Globecom 2010 proceedings.

Transmit Antenna Selection Strategies for Cooperative MIMO AF Relay Networks

Gayan Amarasuriya, Chintha Tellambura and Masoud Ardakani
Department of Electrical and Computer Engineering,
University of Alberta, Edmonton, AB, Canada T6G 2V4
Email: {amarasur,chintha,ardakani}@ece.ualberta.ca

***Abstract*—In this paper, an analytical framework is developed for the performance analysis of three transmit antenna selection (TAS) strategies for dual-hop multiple-input multiple-output channel-assisted amplify-and-forward (CA-AF) relay networks over Rayleigh fading. The cumulative distribution function of a lower bound of the end-to-end signal-to-noise ratio (SNR) of the optimal TAS strategy is derived and used to obtain the upper bounds of the outage probability and the average symbol error rate (SER). The exact moment generating functions (MGFs) of the end-to-end SNR of two suboptimal TAS strategies are also derived for the ideal CA-AF MIMO relay networks. These MGFs are then used to present accurate and efficient closed-form approximations to evaluate the outage probability and average SER. Numerical and Monte-Carlo simulation results are provided to analyze the performance of the system and to verify the accuracy of our analytical framework.**

I. Introduction

Multiple-input multiple-output (MIMO) enabled wireless terminals significantly improve the performance of cooperative relay networks [1]. Transmit antenna selection (TAS) and maximum ratio combining (MRC) can be used effectively to enhance the benefits of such networks [2]. For example, [3]–[6] have investigated these techniques as suboptimal yet simple and efficient beamforming techniques for dual-hop cooperative MIMO relay networks. In this paper, an analytical framework is developed to analyze the performance of MIMO amplify-and-forward (AF) relay networks with TAS over Rayleigh fading.

Prior related research: In [3], the optimal signal-to-noise ratio (SNR)-based TAS strategy (TAS_{opt}) is proposed for dual-hop MIMO AF cooperative relay networks. It is also shown that TAS_{opt} achieves the full diversity order available in the MIMO relay channel. However, the search complexity of TAS_{opt} strategy is relatively high. As a remedy, reference [4] proposes two suboptimal yet low-complexity TAS strategies ($\text{TAS}_{\text{sub-opt}_1}$ and $\text{TAS}_{\text{sub-opt}_2}$) for the same network. Although the performance of these TAS strategies is presented by using Monte-Carlo simulations, no analytical expressions are developed in [4].

The other studies which take into account TAS for dual-hop MIMO relaying are [5] and [6]. In [6], the performance of a dual-hop AF relay network with a MIMO-enabled source-destination pair and a single-antenna relay is analyzed. In this analysis, the source-to-relay ($S \rightarrow R$) and relay-to-destination ($R \rightarrow D$) transmissions take the forms of TAS and MRC, respectively. In [5], three TAS strategies, which are optimal in terms of the outage probability, are developed for MIMO decode-and-forward relaying.

Motivation and our contribution: Although reference [3] derives the diversity order of TAS_{opt}, no closed-form expressions for other performance metrics are derived. However, it compares the average bit error rate (BER) of the binary phase shift keying (BPSK) for TAS_{opt} with several MIMO AF beamforming strategies by using Monte-Carlo simulations. Furthermore, in [4], the performance of the $\text{TAS}_{\text{sub-opt}_1}$ and $\text{TAS}_{\text{sub-opt}_2}$ is not investigated analytically. Instead, the system performance is evaluated in terms of the outage capacity using Monte-Carlo simulations. These gaps in the performance analysis of TAS strategies for MIMO AF relay networks motivated our development of the analytical framework.

In this paper, the cumulative distribution function (CDF) of a lower bound of the end-to-end SNR is derived and used to obtain the upper bounds for the outage probability and the average symbol error rate (SER) of TAS_{opt}. The moment generating functions (MGFs) of the end-to-end SNRs for $\text{TAS}_{\text{sub-opt}_1}$ and $\text{TAS}_{\text{sub-opt}_2}$ are derived as well. Moreover, accurate approximations, which are based on the MGFs, are presented to evaluate the outage probability and the average SER of $\text{TAS}_{\text{sub-opt}_1}$ and $\text{TAS}_{\text{sub-opt}_2}$. In order to obtain valuable insights, the diversity order of the three TAS strategies is summarized. Numerical and Monte-Carlo simulation results are also provided to analyze the performance and to verify the accuracy of our analytical framework.

The rest of this paper is organized as follows: Section II presents the system and the channel model. Section III summarizes the three TAS strategies. In Section IV, the performance analysis is presented. Section V contains the numerical and simulation results. Section VI concludes the paper.

Notations: $\mathcal{K}_\nu(z)$ is the *Modified Bessel function of the second kind of order* ν [7, Eq. (8.407.1)]. ${}_2\mathcal{F}_1(\alpha, \beta; \gamma; z)$ is the *Gauss Hypergeometric function* [7, Eq. (9.14.1)]. $\Re\{z\}$ denotes the real part of z. $\| \mathbf{Z} \|_F$ denotes the *Frobenius norm* of $\mathbf{Z}$. $n \sim \mathcal{CN}(\mu, \sigma^2)$ denotes that n is a *circular symmetric complex Gaussian* distributed random variable with mean μ and variance σ^2.

II. System Model

We consider the dual-hop cooperative relay network with MIMO enabled source (S), relay (R) and destination (D) having N_s, N_r and N_d antennas, respectively (Fig. 1). All terminals operate in the half-duplex mode, and cooperation takes place in two time-slots. Perfect channel state information (CSI) is assumed at R and D. Further, the feedback channels for TAS at S and R are assumed to be perfect. The channel matrix from

978-1-4244-5638-3/10/$26.00 ©2010 IEEE

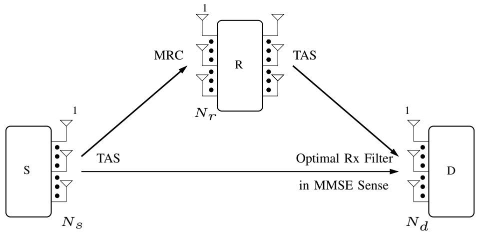

Fig. 1. TAS for MIMO AF relay networks: System Model.

terminal X to terminal Y, where $X \in \{S, R\}, Y \in \{R, D\}$, and $X \neq Y$, is denoted by $\mathbf{H}_{XY}$. The elements of $\mathbf{H}_{XY}$ are independent and identically distributed as $h_{XY}^{i,j} \sim \mathcal{CN}(0,1)$. The channel vector from the j-th transmit antenna at X to Y is denoted by $\mathbf{h}_{XY}^{j}$. Zero mean additive white Gaussian noise is assumed at each receiver.

In the first time-slot, S broadcasts to R and D by selecting a single transmit antenna, and R receives the signal by using MRC. Here, we consider an ideal channel-assisted amplify-and-forward (CA-AF) relay with a gain $G = \frac{1}{\|\mathbf{h}_{SR}^{(i)}\|_F^2}$. In the second time-slot, R amplifies and forwards the received signal to D again by selecting a single transmit antenna. Then D combines the two signals received in the two time-slots by applying the optimal receiver filter in the minimum mean-square error (MMSE) sense [3], [4]. Under this system model, the post-processing end-to-end SNR at D when S and R use the i-th and the k-th transmit antennas is given by

$$\gamma_{eq}^{(i,k)} = \gamma_{SD}^{(i)} + \frac{\gamma_{SR}^{(i)}\gamma_{RD}^{(k)}}{\gamma_{SR}^{(i)} + \gamma_{RD}^{(k)}}, \qquad (1)$$

where $\gamma_{SD}^{(i)} = \bar{\gamma}_0 \| \mathbf{h}_{SD}^{(i)} \|_F^2$, $\gamma_{SR}^{(i)} = \bar{\gamma}_1 \| \mathbf{h}_{SR}^{(i)} \|_F^2$ and $\gamma_{RD}^{(k)} = \bar{\gamma}_2 \| \mathbf{h}_{RD}^{(k)} \|_F^2$ are the equivalent instantaneous SNRs, and $\bar{\gamma}_0$, $\bar{\gamma}_1$, and $\bar{\gamma}_2$ are the average SNRs of the $S \to D$, $S \to R$, and $R \to D$ channels, respectively.

III. Transmit antenna selection (TAS) strategies

For the sake of completeness, this section summarizes the optimal TAS and two suboptimal TAS strategies for the AF MIMO relaying proposed in [3] and [4], respectively.

A. Optimal TAS for AF MIMO relaying (TAS_{opt})

The end-to-end SNR $\gamma_{eq}^{(i,k)}$ for AF MIMO relaying (1) can be maximized by the TAS at S and R as follows [3]: In (1), for fixed $\gamma_{SD}^{(i)}$ and $\gamma_{SR}^{(i)}$, $\gamma_{eq}^{(i,k)}$ is maximized when $\gamma_{RD}^{(k)}$ is maximized; i.e., the TAS at R is independent of the TAS at S. In TAS_{opt}, the antenna indices I and K are selected as

$$K = \underset{1\le k\le N_r}{\text{argmax}}\left(\gamma_{RD}^{(k)}\right) \quad \text{and} \quad I = \underset{1\le i\le N_s}{\text{argmax}}\left(\gamma_{eq}^{(i,K)}\right). \qquad (2)$$

B. Sub-optimal TAS for AF MIMO relaying

The search complexity of TAS_{opt} is considerably high since the transmit antenna at S (i.e., antenna index I in (2)) should be searched to maximize $\gamma_{eq}^{(i,k)}$ by taking into account the both $S \to R$ and $S \to D$ SNRs. Reference [4] proposes two suboptimal TAS strategies, which provide a better trade-off between the search complexity and the performance, as follows:

- $\text{TAS}_{\text{sub-opt}_1}$: TAS is used at S and R separately to maximize the SNR of the $S \to D$ and $R \to D$ channels, respectively.

$$I = \underset{1\le i\le N_s}{\text{argmax}}\left(\gamma_{SD}^{(i)}\right) \ \text{and} \ K = \underset{1\le k\le N_r}{\text{argmax}}\left(\gamma_{RD}^{(k)}\right). \qquad (3)$$

- $\text{TAS}_{\text{sub-opt}_2}$: TAS is used at S and R separately to maximize the SNR of the $S \to R$ and $R \to D$ channels, respectively.

$$I = \underset{1\le i\le N_s}{\text{argmax}}\left(\gamma_{SR}^{(i)}\right) \ \text{and} \ K = \underset{1\le k\le N_r}{\text{argmax}}\left(\gamma_{RD}^{(k)}\right). \qquad (4)$$

IV. Performance Analysis

This section presents the performance analyses of three TAS strategies (2), (3) and (4).

A. Statistical characterization of the end-to-end SNR

1) The CDF of the end-to-end SNR for TAS_{opt}: Let $\gamma_{\text{eq}}^{\text{opt}}$ denote the the end-to-end SNR at D for TAS_{opt}. The CDF of the lower bound for $\gamma_{\text{eq}}^{\text{opt}}$ is given by

$$\begin{aligned} F_{\gamma_{\text{eq,lb}}^{\text{opt}}}(x) = &\Bigg[1 - \sum_{a=1}^{N_s}\sum_{b=0}^{a(N_r-1)}\sum_{p=0}^{N_r-1}\sum_{q=0}^{p(N_d-1)}\sum_{l=0}^{N_d+b+q-1} \frac{2N_r\binom{N_s}{a}\binom{N_r-1}{p}}{\Gamma(N_d)} \\ &\times \frac{\binom{N_d+b+q-1}{l}(-1)^{a+p+1} a^{\frac{l-b+1}{2}} \beta_{b,a,N_r}\beta_{q,p,N_d}}{(p+1)^{\frac{l-b+1}{2}}\bar{\gamma}_1^{\frac{l+b+1}{2}}\bar{\gamma}_2^{\frac{2N_d+2q-l+b-1}{2}}} \\ &\times x^{N_d+b+q}\exp(-x\kappa)\,\mathcal{K}_{l-b+1}(x\lambda)\Bigg] \\ &\times \left[\sum_{m=0}^{N_s}\sum_{n=0}^{m(N_d-1)}\binom{N_s}{m}\frac{\beta_{n,m,N_d}}{\bar{\gamma}_0}x^n\exp\left(-\frac{mx}{\bar{\gamma}_0}\right)\right], \end{aligned} \qquad (5)$$

where $\kappa = \frac{a}{\bar{\gamma}_1} + \frac{p+1}{\bar{\gamma}_2}$, $\lambda = 2\sqrt{\frac{a(p+1)}{\bar{\gamma}_1\bar{\gamma}_2}}$, and $\beta_{k,N,L}$ is the coefficient of the expansion of $\left[\sum_{u=0}^{L-1}\frac{1}{u!}\left(\frac{x}{\bar{\gamma}}\right)^u\right]^N = \sum_{k=0}^{N(L-1)}\beta_{k,N,L}\left(\frac{x}{\bar{\gamma}}\right)^k$ and given by [8, Eq. (44)]

$$\beta_{k,N,L} = \sum_{i=k-L+1}^{k}\frac{\beta_{i,N-1}}{(k-i)!}I_{[0,(N-1)(L-1)]}(i), \qquad (6)$$

$\beta_{0,0,L} = \beta_{0,N,L} = 1$, $\beta_{k,1,L} = 1/\ k!$, $\beta_{1,N,L} = N$ and $I_{[a,c]}(b) = \begin{cases} 1, & a \le b \le c \\ 0, & \text{otherwise} \end{cases}$. The proof can be found in [9].

2) The MGF of the end-to-end SNR for $TAS_{sub\text{-}opt_1}$: Let $\gamma_{\text{eq}}^{\text{sub-opt}_1}$ denote the the end-to-end SNR at D for $\text{TAS}_{\text{sub-opt}_1}$. The MGF of $\gamma_{\text{eq}}^{\text{sub-opt}_1}$ is given by

$$\mathcal{M}_{\gamma_{\text{eq}}^{\text{sub-opt}_1}}(s) = \mathcal{M}_{\gamma_{\text{SRD}}^{\text{sub-opt}_1}}(s)\,\mathcal{M}_{\gamma_{SD}^{\text{sub-opt}_1}}(s), \qquad (7)$$

where $\mathcal{M}_{\gamma_{\text{SRD}}^{\text{sub-opt}_1}}(s)$ and $\mathcal{M}_{\gamma_{SD}^{\text{sub-opt}_1}}(s)$ are the MGFs of the SNRs of relayed path and the direct path. They are given by

$$\begin{aligned} \mathcal{M}_{\gamma_{\text{SRD}}^{\text{sub-opt}_1}}(s) = 1 - &\sum_{a=1}^{N_r}\sum_{b=0}^{a(N_d-1)}\sum_{c=0}^{b+N_r-1}\frac{2(-1)^{a+1}a^{\frac{c-b+1}{2}}\beta_{b,a,N_d}}{\Gamma(N_r)} \\ &\times \frac{\binom{N_r}{a}\binom{b+N_r-1}{c}}{\bar{\gamma}_1^{\frac{2N_r+b-c-1}{2}}\bar{\gamma}_2^{\frac{c+b+1}{2}}}\, s\,\mathbb{I}(\mu,\nu,\psi,\omega), \quad \text{where} \end{aligned} \qquad (8)$$

This full text paper was peer reviewed at the direction of IEEE Communications Society subject matter experts for publication in the IEEE Globecom 2010 proceedings.

$\mathbb{I}(\mu,\nu,\psi,\omega) = \frac{\sqrt{\pi}(2\omega)^{\nu}\Gamma(\mu+\nu)\Gamma(\mu-\nu)\,{}_2\mathcal{F}_1\left(\mu+\nu,\nu+\frac{1}{2};\mu+\frac{1}{2};\frac{\psi-\omega}{\psi+\omega}\right)}{(\psi+\omega)^{\mu+\nu}\Gamma\left(\mu+\frac{1}{2}\right)}$, $\mu = N_r + b + 1$, $\nu = c - b + 1$, $\psi = s + \frac{1}{\bar{\gamma}_1} + \frac{a}{\bar{\gamma}_2}$ and $\omega = 2\sqrt{\frac{a}{\bar{\gamma}_1\bar{\gamma}_2}}$, and

$$\mathcal{M}_{\gamma_{SD}^{\text{sub-opt}_1}}(s) = \sum_{p=0}^{N_s}\sum_{q=0}^{p(N_d-1)} \frac{\binom{N_s}{p}(-1)^p \beta_{q,p,N_d}\bar{\gamma}_0\Gamma(q+1)\, s}{(s\bar{\gamma}_0+p)^{q+1}}. \quad (9)$$

The proof can be found in [9].

3) The MGF of the end-to-end SNR for TAS$_{\text{sub-opt}_2}$: Let $\gamma_{\text{eq}}^{\text{sub-opt}_2}$ denote the the end-to-end SNR at D for TAS$_{\text{sub-opt}_2}$. The MGF of $\gamma_{\text{eq}}^{\text{sub-opt}_2}$ is then given by

$$\mathcal{M}_{\gamma_{\text{eq}}^{\text{sub-opt}_2}}(s) = \mathcal{M}_{\gamma_{\text{SRD}}^{\text{sub-opt}_2}}(s)\,\mathcal{M}_{\gamma_{SD}^{\text{sub-opt}_2}}(s), \quad \text{where} \quad (10)$$

$$\mathcal{M}_{\gamma_{\text{SRD}}^{\text{sub-opt}_2}}(s) = 1 - \sum_{p=1}^{N_r}\sum_{q=0}^{p(N_d-1)}\sum_{a=0}^{N_s-1}\sum_{b=0}^{a(N_r-1)}\sum_{c=0}^{N_r+q+b-1} \frac{2N_s\binom{N_r}{p}}{\Gamma(N_r)} \times \frac{\binom{N_s-1}{a}\binom{N_r+q+b-1}{c}(-1)^{p+q+1}\beta_{q,p,N_d}\beta_{b,a,N_r}}{p^{\frac{q-c-1}{2}}(a+1)^{\frac{c-q+1}{2}}\bar{\gamma}_1^{\frac{2N_r+q+2b-c-1}{2}}\bar{\gamma}_2^{\frac{c+q+1}{2}}}\, s\,\mathbb{I}(\mu,\nu,\psi,\omega), \quad (11)$$

where $\mu = N_r + b + q + 1$, $\nu = c - q + 1$, $\psi = s + \frac{a+1}{\bar{\gamma}_1} + \frac{p}{\bar{\gamma}_2}$ and $\omega = 2\sqrt{\frac{p(a+1)}{\bar{\gamma}_1\bar{\gamma}_2}}$, and

$$\mathcal{M}_{\gamma_{SD}^{\text{sub-opt}_2}}(s) = (1+\bar{\gamma}_o s)^{N_d}. \quad (12)$$

The proof can be found in [9].

B. Outage probability

The outage probability P_{out} is the probability that the instantaneous end-to-end SNR γ_{eq} falls below a threshold γ_{th}; $P_{out} = \Pr(\gamma_{eq} \le \gamma_{th}) = F_{\gamma_{eq}}(\gamma_{th})$, where $F_{\gamma_{eq}}(\gamma_{th})$ denotes the CDF of γ_{eq} evaluated at γ_{th}. An upper bound of P_{out} for TAS$_{\text{opt}}$ can readily be obtained by using (5). Further, P_{out} of TAS$_{\text{sub-opt}_1}$ and TAS$_{\text{sub-opt}_2}$ can accurately be computed by using [10], [11]

$$P_{out}^{\text{sub-opt}_j}\Big|_{j=1}^{2} = F_{\gamma_{eq}^{\text{sub-opt}_j}}(\gamma_{th}) = \frac{1}{5\gamma_{th}}\Psi\left(\frac{2N_p}{5\gamma_{th}}\right)\exp\left(\frac{2N_p}{5}\right) + \frac{2}{5\gamma_{th}}\sum_{k=1}^{N_p-1}\Re\{\exp(\gamma_{th}\Upsilon(\theta_k))\Psi_j(\Upsilon(\theta_k))(1+i\Phi(\theta_k))\} + R_{N_p}, \quad (13)$$

where $\Psi_j(s)|_{j=1}^2 = \mathcal{M}_{\gamma_{eq}^{\text{sub-opt}_j}}(s)/s$, $\theta_k = \frac{\pi k}{N_p}$, $\Upsilon(\theta) = \frac{2N_p}{5\gamma_{th}}\theta(\cot\theta + i)$, $\Phi(\theta) = \theta + (\theta\cot\theta - 1)\cot\theta$, $i = \sqrt{-1}$, and R_{N_p} is the remainder term which is negligible for small N_p such as 20 (see Section V).

C. Average symbol error rate

The conditional error probability (CEP) of the coherent binary phase shift keying (BPSK) and M-ary pulse amplitude modulation (PAM) can be expressed as $P_e|\gamma = \alpha\mathcal{Q}(\sqrt{\beta\gamma})$, where α and β are modulation-dependent constants. The average SER can be derived by integrating CEP $P_e|\gamma$ over the PDF of the SNR γ_{eq}. Thus, an upper bound for the average SER of TAS$_{\text{opt}}$ can be derived by substituting (5) into $\bar{P}_e = \frac{\alpha}{2}\sqrt{\frac{\beta}{2\pi}}\int_0^\infty x^{-\frac{1}{2}}e^{-\frac{\beta x}{2}}F_{\gamma_{eq}}(x)\,dx$ and solving the resulting integral by using [7, Eq. (6.621.3)] as follows:

$$\bar{P}_{e,ub}^{\text{TAS}_{\text{opt}}} = \sum_{m=0}^{N_s}\sum_{n=0}^{m(N_d-1)} \frac{\alpha 2^{n-1}(-1)^m\binom{Ns}{m}\sqrt{\beta\bar{\gamma}_0}\beta_{n,m,N_d}\Gamma(n+\frac{1}{2})}{\sqrt{\pi}(2m+\beta\bar{\gamma}_0)^{n+\frac{1}{2}}} - \sum_{a=1}^{N_s}\sum_{b=0}^{a(N_r-1)}\sum_{p=0}^{N_r-1}\sum_{q=0}^{p(N_d-1)}\sum_{l=0}^{N_d+b+q-1}\sum_{m=0}^{N_s}\sum_{n=0}^{m(N_d-1)} \frac{\alpha a^{\frac{\varsigma}{2}}\sqrt{\beta}N_r}{\sqrt{2\pi}\Gamma(N_d)} \times \frac{\binom{N_s}{a}\binom{N_s}{m}\binom{N_r-1}{p}\binom{N_d+b+q-1}{l}(-1)^{a+p+m+1}}{\bar{\gamma}_0^n\bar{\gamma}_1^{\frac{l+b+1}{2}}\bar{\gamma}_2^{\frac{2N_d+2q+b-l-1}{2}}(p+1)^{\frac{\varsigma}{2}}(\psi+\omega)^{\mu+\nu}}\mathbb{I}(\mu,\nu,\psi,\omega), \quad (14)$$

where $\mu = N_d + b + n + q + \frac{1}{2}$, $\nu = l - b + 1$, $\psi = \frac{\beta}{2} + \frac{m}{\bar{\gamma}_0} + \frac{a}{\bar{\gamma}_1} + \frac{p+1}{\bar{\gamma}_2}$ and $\omega = 2\sqrt{\frac{a(p+1)}{\bar{\gamma}_1\bar{\gamma}_2}}$.

The CEP can also be expressed in an alternative form [12]: $P_e|\gamma = \alpha\mathcal{Q}(\sqrt{\beta\gamma}) = \frac{\alpha}{\pi}\sqrt{\frac{\beta}{2}}\int_0^\infty \frac{\exp(-\gamma(s^2+\beta/2))}{s^2+\beta/2}ds$. By using the variable transformation $s^2+\beta/2 = \beta/(\gamma+1)$, the average SER can be written as $\bar{P}_e = \frac{\alpha}{\pi}\sqrt{\frac{\beta}{2}}\int_0^\infty \frac{M_{\gamma_{\text{eq}}}(s^2+\beta/2))}{s^2+\beta/2}ds = \frac{\alpha}{2\pi}\int_{-1}^{1}\frac{M_{\gamma_{\text{eq}}}(\beta/(\gamma+1))}{\sqrt{1-\gamma^2}}d\gamma$ [12]. Then we use the accurate and computationally efficient method proposed in [12], which uses the Gauss-Chebysheve approximation [13] to obtain a compact closed-form approximation for the average BER of TAS$_{\text{sub-opt}_1}$ and TAS$_{\text{sub-opt}_2}$ as follows:

$$\bar{P}_e^{\text{TAS}_{\text{sub-opt}_j}}\Big|_{j=1}^{2} = \frac{\alpha}{2N_p}\sum_{k=1}^{N_p}\mathcal{M}_{\gamma_{\text{eq}}^{\text{TAS}_{\text{sub-opt}_j}}}\left(\frac{\beta}{2}\sec^2(\theta_k)\right) + R_{N_p}, \quad (15)$$

where N_p is a small positive integer, $\theta_k = \frac{(2k-1)\pi}{4N_p}$, and R_{N_p} is the remainder term. R_{N_p} becomes negligible as N_p increases, even for small values such as 10 (see Section V).

D. Diversity Order

TAS$_{\text{opt}}$ has been shown to provide the maximum achievable diversity order (G_d) of cooperative MIMO AF relay networks; $G_d^{\text{TAS}_{\text{opt}}} = N_sN_d + N_r\min(N_s,N_d)$ [3]. The G_d of dual-hop MIMO relaying without considering the direct transmission is governed by the minimum G_d available in each hop; $G_d = \min(G_d^{SR}, G_d^{RD})$ [14]. By following this result, G_d of TAS$_{\text{sub-opt}_1}$ and TAS$_{\text{sub-opt}_2}$ can be written as

$$G_d^{\text{TAS}_{\text{sub-opt}_1}} = N_sN_d + N_r \text{ and } G_d^{\text{TAS}_{\text{sub-opt}_2}} = N_d + N_r\min(N_s,N_d). \quad (16)$$

In Table I, the G_d of each TAS strategy is presented for several special cases to obtain valuable insights. It shows that when $N_s = 1$, G_d is the same for all three strategies. Moreover, if the destination is equipped with one antenna ($N_d = 1$), then TAS$_{\text{opt}}$ and TAS$_{\text{sub-opt}_1}$ provide the same diversity order. Thus, TAS$_{\text{sub-opt}_1}$ is a better choice than the

TABLE I
DIVERSITY ORDERS OF THE THREE TAS STRATEGIES

TAS Strategy	Diversity Order			
	$N_s=1$	$N_r=1$	$N_d=1$	$N_s=N_r=N_d=N$
TAS$_{\text{opt}}$	N_r+N_d	$N_sN_d+\min(N_s,N_d)$	N_s+N_r	$2N^2$
TAS$_{\text{sub-opt}_1}$	N_r+N_d	N_sN_d+1	N_s+N_r	$N(N+1)$
TAS$_{\text{sub-opt}_2}$	N_r+N_d	$N_d+\min(N_s,N_d)$	N_r+1	$N(N+1)$

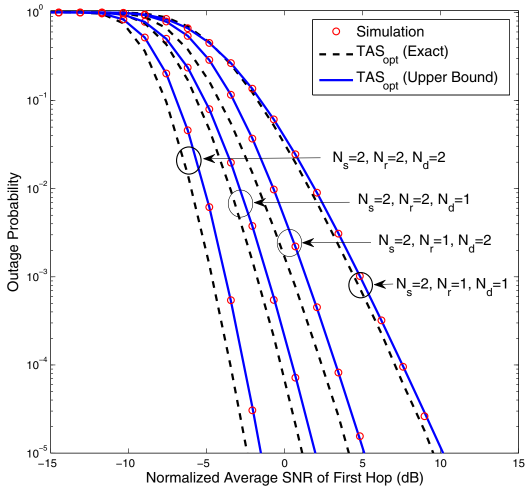

Fig. 2. The outage probability of TAS_{opt} strategy for AF MIMO relay networks. $d_1 = \frac{d_{SD}}{3}, d_2 = \frac{2d_{SD}}{3}$ and $\eta = 2.5$.

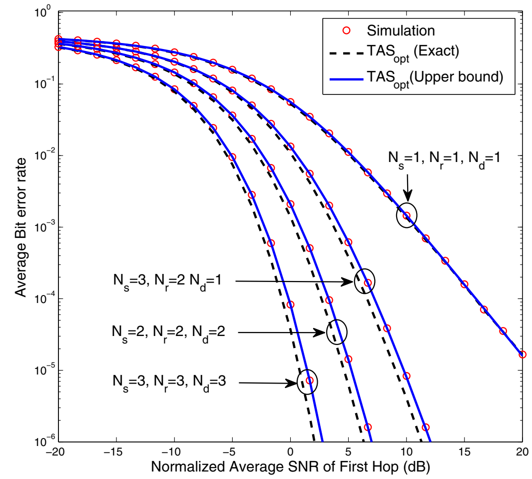

Fig. 3. The average BER of TAS_{opt}, $\text{TAS}_{\text{sub-opt}_1}$ and $\text{TAS}_{\text{sub-opt}_2}$ strategies for AF MIMO relay networks. $d_1 = \frac{d_{SD}}{3}, d_2 = \frac{2d_{SD}}{3}$ and $\eta = 2.5$.

highly complex TAS_{opt} whenever $N_d = 1$. When the number of antennas at each node is the same, the G_d provided by the both $\text{TAS}_{\text{sub-opt}_1}$ and $\text{TAS}_{\text{sub-opt}_2}$ is identical. In practice, the direct channel may be fully unavailable due to heavy shadowing. In this case, the diversity orders of the three strategies are given by $G_d^{\text{TAS}_{\text{opt}}} = G_d^{\text{TAS}_{\text{sub-opt}_2}} = N_r \min(N_s, N_d)$ and $G_d^{\text{TAS}_{\text{sub-opt}_1}} = N_r$. Thus, $\text{TAS}_{\text{sub-opt}_2}$ is a better choice than the others since it always provides better G_d than $\text{TAS}_{\text{sub-opt}_1}$, and the same G_d as in TAS_{opt}.

Remark IV.1: In dual-hop MIMO AF relaying, when the direct path is not taken into account, the optimal TAS strategy is to select the antenna indices I and K at S and R to maximize the SNRs of $S \to R$ and $R \to D$ channels; $I = \underset{1\le i\le N_s}{\operatorname{argmax}}\left(\gamma_{SR}^{(i)}\right)$ and $K = \underset{1\le k\le N_r}{\operatorname{argmax}}\left(\gamma_{RD}^{(k)}\right)$. Thus, the CDF of the end-to-end SNR $\gamma_{\text{eq}}^{\text{opt}}$ of the optimal TAS for dual-hop MIMO AF relaying, when the direct path is ignored, is given by (see [9] for the proof)

$$F_{\gamma_{\text{eq}}^{\text{opt}}}(x) = \sum_{p=1}^{N_r} \sum_{q=0}^{p(N_d-1)} \sum_{a=0}^{N_s-1} \sum_{b=0}^{a(N_r-1)} \sum_{c=0}^{N_r+q+b-1} \frac{2N_s\binom{N_r}{p}}{\Gamma(N_r)} \times \frac{\binom{N_s-1}{a}\binom{N_r+q+b-1}{c}(-1)^{p+q+1}\beta_{q,p,N_d}\beta_{b,a,N_r}}{(a+1)^{\frac{c-q+1}{2}}\bar{\gamma}_1^{\frac{2N_r+2b+q-c-1}{2}}\bar{\gamma}_2^{\frac{c+q+1}{2}}} \times p^{\frac{c-q+1}{2}} x^{N_r+b+q}\exp(-\delta x)\mathcal{K}_{c-q+1}(\epsilon x), \quad (17)$$

where $\delta = \frac{a+1}{\bar{\gamma}_1} + \frac{p}{\bar{\gamma}_2}$ and $\epsilon = 2\sqrt{\frac{p(a+1)}{\bar{\gamma}_1\bar{\gamma}_2}}$. The corresponding MGF of $\gamma_{\text{eq}}^{\text{opt}}$ is given by (11). Further, the average SER is given by

$$\bar{P}_e = \frac{\alpha}{2} - \frac{\alpha}{2}\sqrt{\frac{\beta}{2\pi}} \sum_{p=1}^{N_r} \sum_{q=0}^{p(N_d-1)} \sum_{a=0}^{N_s-1} \sum_{b=0}^{a(N_r-1)} \sum_{c=0}^{N_r+q+b-1} \frac{2N_s\binom{N_r}{p}}{\Gamma(N_r)} \times \frac{\binom{N_s-1}{a}\binom{N_r+q+b-1}{c}(-1)^{p+q+1}\beta_{q,p,N_d}\beta_{b,a,N_r}}{p^{\frac{q-c-1}{2}}(a+1)^{\frac{c-q+1}{2}}\bar{\gamma}_1^{\frac{2N_r+2b+q-c-1}{2}}\bar{\gamma}_2^{\frac{c+q+1}{2}}} \mathbb{I}(\mu,\nu,\psi,\epsilon), \quad (18)$$

where $\mu = N_r + b + q + 1/2$, $\nu = l - q + 1$, and $\psi = \frac{\beta}{2} + \frac{a+1}{\bar{\gamma}_1} + \frac{p}{\bar{\gamma}_2}$.

V. Numerical Results

This section verifies our analysis through Monte-Carlo simulations. To capture the effect of network geometry, the average SNR of the i-th hop is modeled by $\bar{\gamma}_i|_{i=1}^2 = \bar{\gamma}_0\left(\frac{d_{SD}}{d_i}\right)^\eta$, where $\bar{\gamma}_0$ and η are the average SNR of direct path and path-loss exponent. Parameters d_{SD} and d_i are defined as the distance between the source-destination pair and distance between the nodes in the two hop.

Fig. 2 compares the exact and the closed-form upper bound (5) for the outage probability of TAS_{opt}. The exact outage probability is plotted by using Monte-Carlo simulations. This figure shows the tightness of our bound for different antenna configurations at S, R and D. Our upper bound is approximately 1 dB within the exact in the useful SNRs and provides accurate insights about the important system parameters such as the diversity order.

Similarly in Fig. 3, the closed-form upper bound for the average BER of BPSK for TAS_{opt} is compared for different antenna configurations at S, R and D. As our BER bound too is always exact within 1 dB, it may be useful as a benchmark for MIMO dual-hop AF relay network designing.

Fig. 4 compares the average BER of BPSK of the three TAS strategies and also shows the impact of different antenna configurations on the average BER. The exact average BER of TAS_{opt} is evaluated by using Monte-Carlo simulation; while those of $\text{TAS}_{\text{sub-opt}_1}$ are computed by using (15) with $R_{N_p} = 10$. Further, the average BER of a relay network with single-antenna nodes (i.e., $N_s = N_r = N_d = 1$) is also plotted as a benchmark to illustrate the performance gain obtained by TAS for AF MIMO relaying. $\text{TAS}_{\text{sub-opt}_1}$ always performs better than $\text{TAS}_{\text{sub-opt}_2}$ for the given antenna setups. $\text{TAS}_{\text{sub-opt}_1}$ performs approximately similarly to TAS_{opt} in terms of BER when D is equipped with a single-antenna. $\text{TAS}_{\text{sub-opt}_1}$ is thus a better choice than the highly complex TAS_{opt} for networks with $N_d = 1$; while $\text{TAS}_{\text{sub-opt}_2}$ performs considerably poorer than the other two schemes. The exact

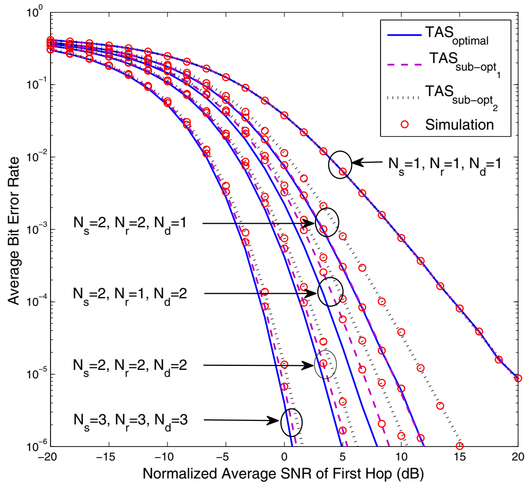

Fig. 4. The average BER of TAS_{opt}, $\text{TAS}_{\text{sub-opt}_1}$ and $\text{TAS}_{\text{sub-opt}_2}$ strategies for AF MIMO relay networks. $d_1 = \frac{d_{SD}}{3}, d_2 = \frac{2d_{SD}}{3}$ and $\eta = 2.5$.

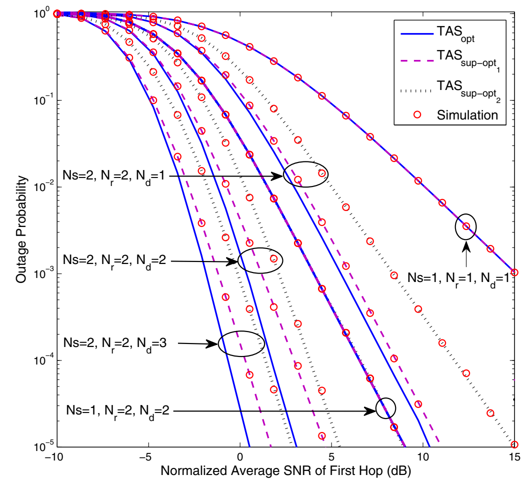

Fig. 5. The outage probability of TAS_{opt}, $\text{TAS}_{\text{sub-opt}_1}$ and $\text{TAS}_{\text{sub-opt}_2}$ strategies for AF MIMO relay networks. $d_1 = d_2 = d_{SD}$ and $\eta = 2.5$.

agreement between the Monte-Carlo simulation points and the analytical results verify the accuracy of our closed-form average BER approximations.

Similarly, Fig. 5 shows the outage probability of the three TAS strategies for different antenna set-ups. The exact outage probability of TAS_{opt} is computed again using Monte-Carlo simulations; while those of $\text{TAS}_{\text{sub-opt}_1}$ and $\text{TAS}_{\text{sub-opt}_2}$ are obtained using (13) with $R_{N_p} = 20$. Fig. 5 shows the impact of number of antennas at D on the outage probability for a fixed number of antennas at S and R. As expected, the TAS_{opt} outperforms the other TAS strategies at the expense of higher search complexity for antenna indices. Whenever, S is equipped with a single-antenna, the performance of the three TAS strategies is identical. This insight thus shows that any of the three strategies can effectively be used for $S \to R \to D$ up-link, where S is usually a mobile device equipped with a single-antenna due to power and space constrains. Similarly, $\text{TAS}_{\text{sub-opt}_1}$ can be used instead of TAS_{opt} for $D \to R \to S$ down-link as both of them provide the same diversity order whenever $N_d = 1$. The Monte-Carlo simulation results agree well with our closed-form outage probability approximation verifying its accuracy.

VI. Conclusion

An analytical framework was developed for the performance analysis of three TAS strategies for dual-hop MIMO CA-AF relay networks. The CDF of a lower bound of the end-to-end SNR was derived and used to obtain the upper bounds of the outage probability and the average SER for TAS_{opt}. The exact MGFs of the end-to-end SNR of $\text{TAS}_{\text{sub-opt}_1}$ and $\text{TAS}_{\text{sub-opt}_2}$ were derived for the ideal CA-AF MIMO relay networks. Closed-form approximations were also presented to evaluate the outage probability and the average SER accurately. The diversity orders of TAS strategies were summarized to get valuable insights. Monte-Carlo simulations were provided to validate the accuracy of our analytical developments. The numerical results show that significant performance gains can be achieved using TAS in MIMO AF relaying. Our analytical framework may be used to obtain valuable insights into the designing MIMO AF relay networks with TAS.

References

[1] Y. Fan and J. Thompson, "MIMO configurations for relay channels: Theory and practice," *IEEE Trans. Wireless Commun.*, vol. 6, no. 5, pp. 1774–1786, May 2007.

[2] S. Thoen, L. Van der Perre, B. Gyselinckx, and M. Engels, "Performance analysis of combined transmit-SC/receive-MRC," *IEEE Trans. Commun.*, vol. 49, no. 1, pp. 5 – 8, Jan 2001.

[3] S. Peters and R. W. Heath, "Nonregenerative MIMO relaying with optimal transmit antenna selection," *IEEE Signal Process. Lett.*, vol. 15, pp. 421–424, 2008.

[4] L. Cao, X. Zhang, Y. Wang, and D. Yang, "Transmit antenna selection strategy in amplify-and-forward MIMO relaying," in *Wireless Communications and Networking Conference, IEEE*, Budapest, Apr. 2009.

[5] A. Muller and J. Speidel, "Outage-optimal transmit antenna selection for cooperative decode-and-forward systems," in *Vehicular Technology Conference, 2009. VTC Spring 2009. IEEE 69th*, Apr 2009, pp. 1 –5.

[6] S. Chen, W. Wang, X. Zhang, and D. Zhao, "Performance of amplify-and-forward MIMO relay channels with transmit antenna selection and maximal-ratio combining," in *Wireless Communications and Networking Conference, 2009. IEEE*, Apr 2009.

[7] I. Gradshteyn and I. Ryzhik, *Table of integrals, Series, and Products*, 7th ed. Academic Press, 2007.

[8] A. Annamalai and C. Tellambura, "Error rates for Nakagami-m fading multichannel reception of binary and M-ary signals," *IEEE Trans. Commun.*, vol. 49, no. 1, pp. 58–68, Jan. 2001.

[9] G. Amarasuriya, C. Tellambura, and M. Ardakani, "Transmit antenna selection strategies for cooperative MIMO AF relay networks," *IEEE Trans. Wireless Commun.*, 2010, (submitted).

[10] J. Abate and P. P. Valko, "Multi-precision laplace transform inversion," *"International J. Numerical Methods in Engineering"*, vol. 60, no. 5, pp. 979–993, May 2004.

[11] R. C. Palat, A. Annamalai, and J. H. Reed, "An efficient method for evaluating information outage probability and ergodic capacity of OSTBC system," *IEEE Commun. Lett.*, vol. 12, no. 3, pp. 191–193, Mar. 2008.

[12] A. Annamalai, C. Tellambura, and V. K. Bhargava, "Efficient computation of MRC diversity performance in Nakagami fading channel with arbitrary parameters," *Electronics Letters*, vol. 34, no. 12, pp. 1189–1190, Jun. 1998.

[13] M. Abramowitz and I. Stegun, *Handbook of Mathematical Functions*. Dover Publications, Inc., New York, 1970.

[14] M. Yuksel and E. Erkip, "Multiple-antenna cooperative wireless systems: A diversity-multiplexing tradeoff perspective," *IEEE Trans. Inf. Theory*, vol. 53, no. 10, pp. 3371 –3393, oct. 2007.